CNRS

Centre National de la Recherche Scientifique

INFN

Istituto Nazionale di Fisica Nucleare

Commissioning progress report for the STAC and the EGO council

VIR-043A-08

Issue: 1

Date: May 30, 2008

The Virgo Collaboration

VIRGO * A joint CNRS-INFN Project
Via E. Amaldi, I-56021 – S. Stefano a Macerata - 56021 Cascina, Italia.
Secretariat: Telephone.(39) 050 752 521 * FAX.(39) 050 752 550 * e-mail virgo@virgo.infn.it

1 Introduction

After the end of the first Virgo science run (VRS1) the commissioning activity was dedicated to the reduction of the control noises which were limiting the sensitivity typically below 50 Hz, and to the understanding and then the reduction of environmental noises (beam jitter, diffused light and magnetic noise), limiting the sensitivity up to few 100 Hz. Finally, when the thermal compensation was ready it has been installed and commissioned.

During the first months the commissioning activity was first focused on the reduction of the control noises (see sections 1.3.1 and 1.3.2). All control noises are now very close to the Virgo design sensitivity. These improvements also resulted in a much more robust lock of the interferometer.

Then the activity concentrated on the understanding and the reduction of environmental noises and their coupling to the dark fringe. These concerned magnetic noise, beam jitter and diffused light (see section 1.5). Hardware modifications were necessary for the reduction of some of these noises, leading to shutdown periods of few days to one week. These hardware modifications concerned the replacement of the injection beam monitoring system (beam jitter reduction), the replacement of the optical setup of the end benches (diffused light reduction), the replacement of the detection Brewster window with a cryogenic trap (diffused light reduction) and the replacement of the mirrors' magnets with smaller ones (magnetic noise coupling and Eddy currents reduction). The known environmental noises are now all very close to the design sensitivity.

Finally, when the thermal compensation system (TCS) was ready it has been installed mid-April (10 days shutdown). Unfortunately one CO_2 laser was not working and the compensation was therefore available only for one of the input mirrors (WI). The last month of commissioning was dedicated to the TCS commissioning (with only one CO_2 laser) and to the reduction of diffused light on external optical benches.

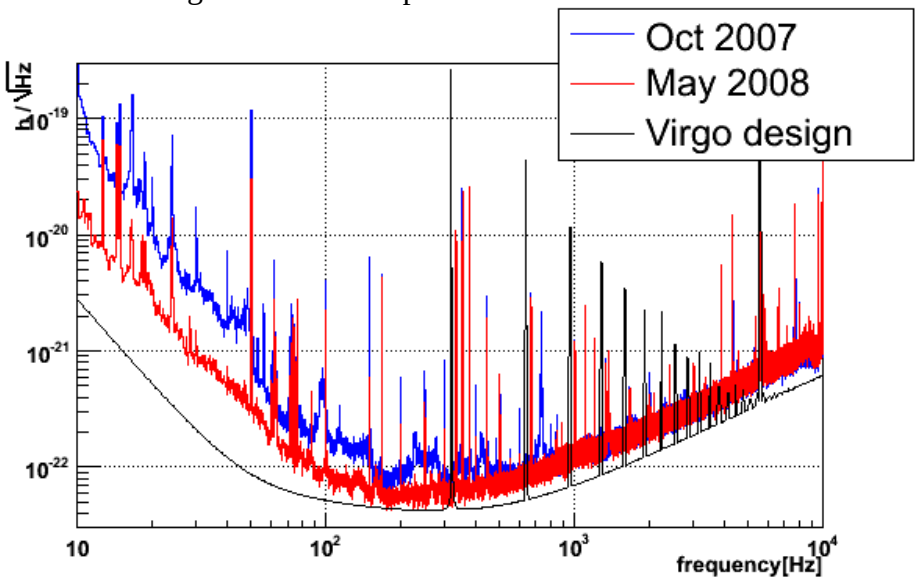

Fig 1: *Comparison of the sensitivities at the time of the last report (Oct 9th) and on May 5th just before the shutdown.*

The activity has been interrupted 3 weeks before originally planned due to the incident at NE (see Detector report). This happened just at the end of the replacement of the magnets of the end mirrors aimed at a reduction of magnetic noise and possibly of the Eddy currents. This incident prevented from completing the commissioning of the Virgo with TCS and from checking the effect of using smaller magnets. Nevertheless encouraging results have been obtained in terms of thermal compensation (see section 1.4). The activities which were planned for these last three weeks were: the installation of the second TCS laser, the installation of the phase camera system and the commissioning of the full TCS system. It was also planned to further reduce the impact of diffused light on optical benches, and characterize the impact of other optical elements (injection Brewster, towers output windows).

Figure 1 shows a comparison of the sensitivity at the time of the last report (Oct 9th) and the most recent one (May 5th). Section 1.6 summarizes the understanding of the noises contributing to the sensitivity and the plans for further reduction.

The commissioning of the interferometer will restart at the end of this summer and until the start of VSR2 with the commissioning of the new injection system (see 1.3.4) and of the new control electronics (see 1.2), the completion of the thermal compensation together with the increase of the input power and further reduction of noises at low frequency (see section 1.7).

2 Detector operation, electronic and software

2.1 Detector operation

From the time of the last report, the Detector Operation activities were mainly devoted to provide the usual daily support/troubleshooting in the Control Room (operator service, monitoring tools, training and procedures) and to the implementation of the Auto-Relock described here.

The Auto-Relock was implemented in order to have the ITF locked as much as possible when left unattended (ie at night and weekends) to contribute to the astrowatch program and to collect data for commissioning studies. Such implementation, although conceptually simple thanks to the architecture on which the automation is based, has not been straightforward, due to safety reasons, and to some missing functionality in the automation code (ALP) to deal with exceptions (crash of server, missing channel). After the implementation and deployment of a new ALP version featuring the functionality to recognize and manage the exceptions the dedicated procedure and macros were implemented. When the auto-relock is engaged, in case of unlock ALP tries to relock and in case of SW/HW exception or impossibility to lock after *n* consecutive attempts, the ITF is brought to the lock acquisition pre-conditions and the failure is notified to the on-call person. The first use of the auto-relock was during the Christmas period: the ITF was left unattended and the on-call service was always active. The result of the test, summarized in Fig.2, has been satisfactory also thanks to the on-call intervention to recover a major HW failure. Since the beginning of the year, the auto-relock is normally engaged when leaving before night and weekend. It happens that in case of failure (and automatic notification), the duty-cycle is lowered also because the on-call service is not active during night and weekend. The level of automation so far implemented is a key element to speed-up the commissioning activity and to enhance the astrowatch capability out of the commissioning or upgrade periods: since VSR1 stop, duty-cycle is ~40% and 12% for ITF locked and Science Mode, respectively.

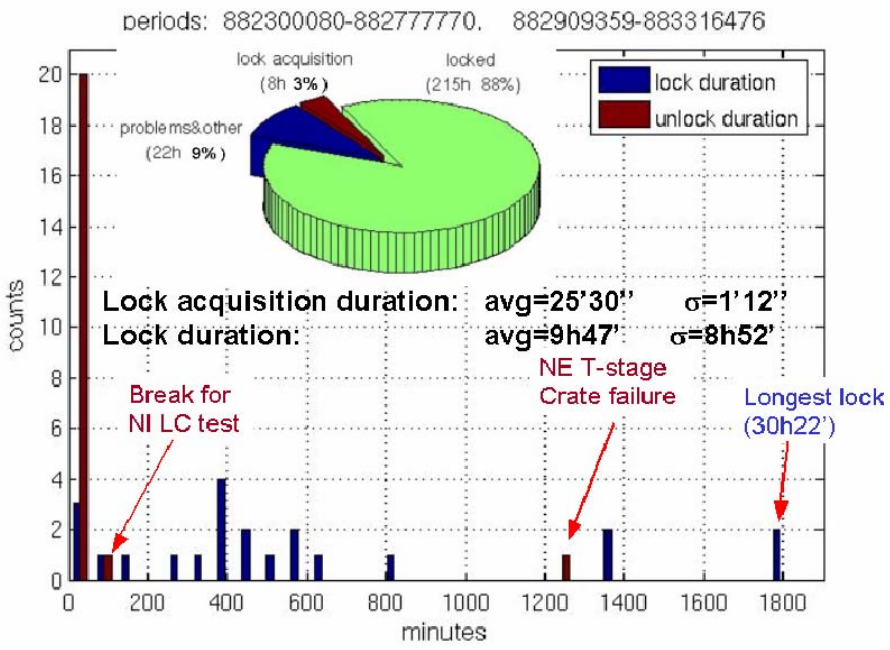

Fig. 2: Statistics of the 245 hours long test on auto-relock performed during the Christmas period. The bar graph displays the distribution of the duration of the lock and unlock periods; the pie chart displays the duty-cycle, the downtime percentage and the time spent for the lock acquisition.

2.2 Electronic and software

Many Electronic and Software activities have been performed spanning over different subsystems as reported in this document on the dedicated sections. To be worth mentioning:

- New coil driver boards: tests on ITF completed including the driving with smaller magnets. The final production is starting.
- Galvanometers: driving electronic has been completed and installed
- Cryogenic trap: control electronic and control/data acquisition software has successfully been put in operation
- Thermal Compensation: whole control electronic and software including in vacuum mirror steering and motorized wave plate for power tuning successfully put in operation on WI bench.

Current developments and plans:

The major efforts are focused on the updates associated to the Virgo+ Control and DAQ electronics and the porting of the associated software: Global control (Gc), Photodiode Readout (Pr), etc.
One of the preparatory activities has been the development of an integration database provided with a web interface in order to trace efficiently the deployment of the electronics. This database will also contain the TOLM network configuration.
It should be stressed that the new architecture has been conceived so that it can be put in operation step by step in parallel with the current architecture. The installation will take place from June to August as well as functional tests like the computing with the new Pr-Gc with signals acquired with old and new ADCs. A provisional plan for the commissioning with the ITF is the following:

1/ Use the new ADC for the monitoring channels before the commissioning restart and validate them

2/ Relock the ITF with the old Virgo control system. The ITF signals will also feed the new ADCs and new readout/control software (Pr, Gc) so that the whole chain can be validated during lock acquisition by comparing the control signals of the 2 chains.
3/ Lock the ITF with the new system (from the ADCs to the global control system). An intermediate step to be considered is to keep using the old ADCs while putting in operation and validating the new software.
4/ When available, install 1 new DSP on the upper part of a suspension for validation.
5/ Replace the lower stage DSPs on all towers.

3 Interferometer control

3.1 Longitudinal control

The activities concerning the longitudinal control system have focused mainly in a first campaign of system characterization experiments, which lately allowed a large improvement in the stability and noise performances of the system. Figure 3 compares a typical longitudinal noise budget of October 2007 with one from May 2008. The main improvements with respect to VSR1 configuration were: the use of 8MHz signal and of a new sensing scheme for the central interferometer control; the optimization of control filters to improve low frequency accuracy and reduce high frequency noise re-introduction; the improvement of noise subtraction techniques. All these improvements required a large campaign of modification and optimization of the global control locking code.

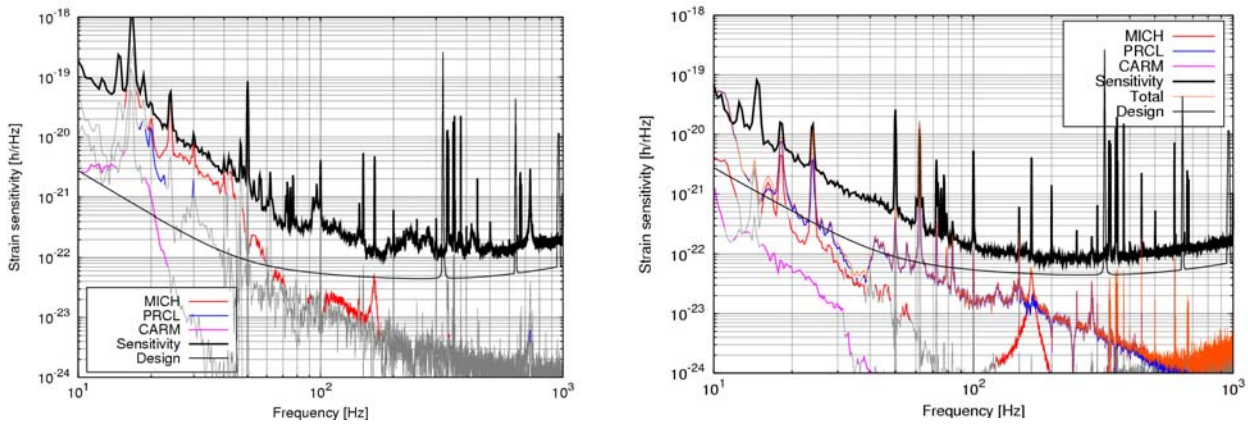

Fig. 3. *Comparison between a typical longitudinal noise budget of October 2007 (left) and of May 2008 (right). After the improvements in the longitudinal control system described in the text, control noise is no more limiting the sensitivity and it is almost complaint with Virgo design.*

New sensing strategy

The central interferometer degrees of freedom (short Michelson differential motion MICH and power recycling cavity length PRCL) were during the run the critical ones in terms of control noise re-introduction. A first campaign of measurements devoted to ITF characterization and the implementation of the phase-locked 8 MHz modulation allowed changing the error signals used for these d.o.f.s. Table 1 summarizes the VSR1 and new sensing schemes. The main improvement comes from the use of the less noisy B2 8MHz signal for MICH control: the net result of this modification alone allowed reducing MICH correction by about one order of magnitude everywhere above 10 Hz, see Figure 4.

	Old (VSR1) configuration	New sensing scheme
MICH		
Error signal	B5_Q + B2_6MHz_P + B2_18MHz_P (< 5 Hz)	B2_8MHz_P
UGF	15 Hz	10 Hz
PRCL		
Error signal	B2_6MHz_P + B2_18MHz_P (< 5 Hz)	B5_Q
UGF	40 Hz	80 Hz

Table 1. *Comparison of the VSR1 and new sensing scheme for longitudinal control.*

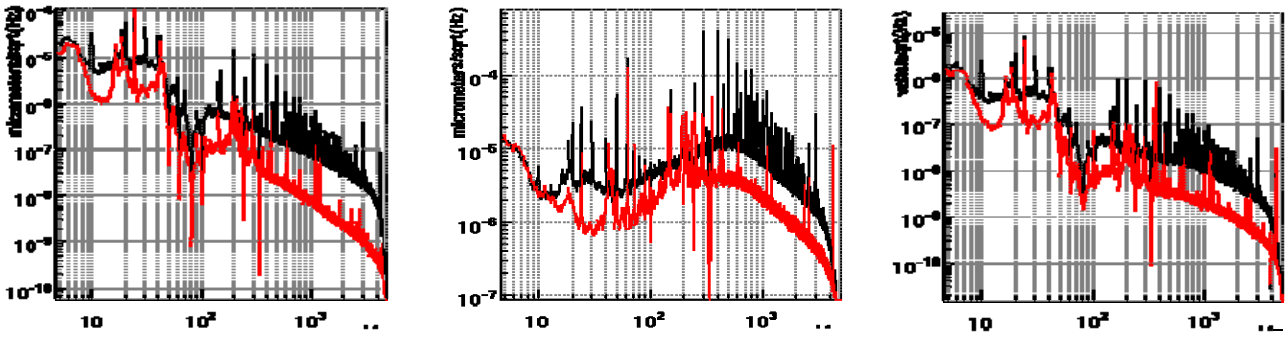

Fig.4. *Comparison of MICH, PRCL and end mirror correction with the VSR1 (black) and new (red) sensing scheme. The reduction is significant for all frequencies above 10 Hz.*

Control filter improvements

The filters used for the control of the four longitudinal degrees of freedom (MICH, PRCL, differential arm DARM and common arm CARM) were largely modified in order to:

- increase the low frequency gain. PRCL residual motion has been reduced by more than one order of magnitude and MICH one by more than a factor 3.
- improve the high frequency (above 10 Hz) roll-off of MICH to reduce re-introduction of control noise
- have a better balancing of phase and gain margins for the DARM loop. In particular the phase margin of this loop was very low, resulting in a large gain peaking around 100 Hz in the closed loop transfer function. This directly affected the sensitivity calibration curve, which could change by up to 30% due to input mirror etalon effects. After the filter modification the expected variation due to the same effect is less then 3%.

Noise subtraction techniques

The coupling of auxiliary loops (MICH, PRCL and CARM) correction to the dark fringe signal is pretty large. For this reason noise subtraction techniques have been implemented: correction signals are filtered and added to the DARM one, in order to cancel the normal noise coupling. Before and during the run only MICH and PRCL noise subtraction was implemented. After the already mentioned control noise improvements, CARM noise started to be limiting, and therefore another noise subtraction has been added.
The technique used for measuring the optimal (frequency-dependent) subtraction coefficient has been largely improved, resulting in normal noise suppression factors of about 1000 for MICH: this means that the contribution to dark fringe of MICH noise is normally reduced by

this factor by means of the subtraction technique. Lower accuracy were needed for PRCL (about 10) and CARM (about 100).

Locking with TCS and plans

Once the thermal compensation has been installed the locking activity was focused on locking the ITF with TCS, results are reported in 1.4.2. This activity will go on after the Virgo+ shutdown starting from the same input power (~8 Watts). If it turns out to be impossible to obtain a good thermal compensation starting from this power it might be needed to lock the ITF with a low power (few Watts) in order to start from a state with well reduced aberrations. In that case the lock of the ITF will have to be re-commissioned with low input power and to handle the slow (but large) input power increase (few Watts to 25 Watts) during the lock of the ITF.

3.2 Angular control

The figure 5 gives an overview of the last alignment configuration used. Demodulated signals (wavefront sensing) are used for controlling beam splitter, power recycling, and differential end mirror alignment, and the input beam angle. The common end mirror alignment is controlled by the position of the beam reflected by the interferometer (B2, DC asymmetry signal). The input mirrors are controlled by injecting a sinusoidal perturbation on the end mirror alignment, and minimizing its effect on the dark fringe. In this way an optimal centring of the beam on the end mirrors (minimum coupling of alignment noise to length) is assured.

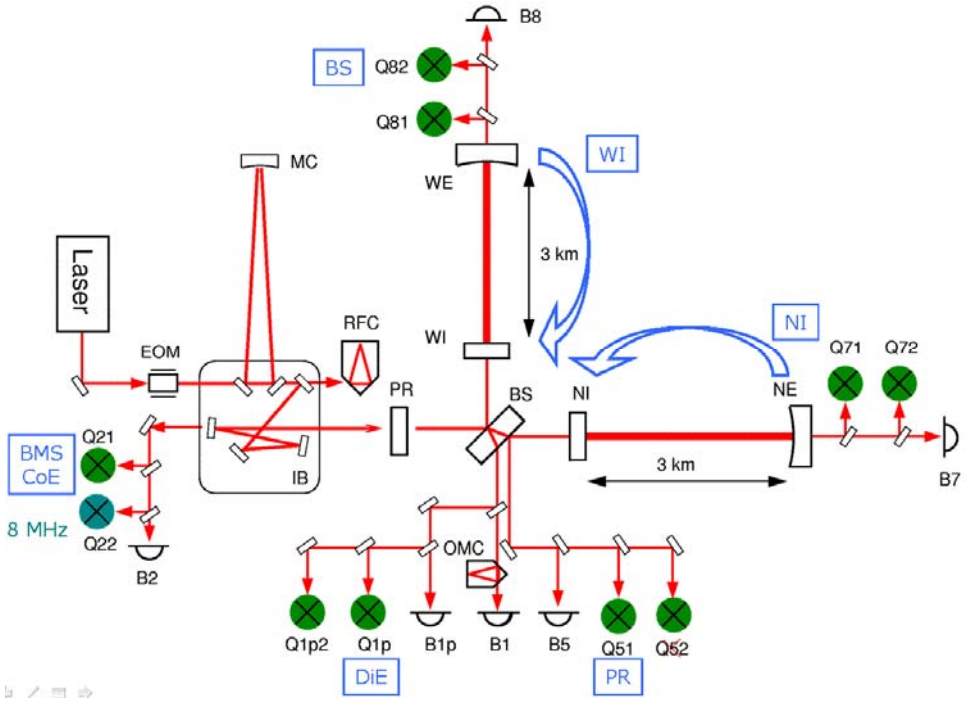

Fig. 5: Virgo alignment layout. The blue rectangles show the degrees of freedom controlled with each quadrant diode (green circles). NI/WI = North/West input mirrors; BS = beam splitter; PR = Power recycling mirror; BMS = input beam steering system; CoE,DiE = Common/Differential End mirror motion. NI/WI are controlled with signals giving the miscentering of the beam on the end mirrors.

The optical setup of the North and West terminal benches has been upgraded in order to improve the beam quality (less spherical aberrations), reduce the number of optical components and improve their arrangement for reducing scattered light effects, and improve the setup of the quadrant diodes (better Gouy phase settings). This has allowed to have better

error signals for the beam splitter alignment, but most of the terminal quadrant diode signals are still too noisy, especially at low frequency (0.01…20 Hz) in order to be useful. We are investigating the impact of air currents, which might be mitigated by plexiglass covers on the concerned optical benches, on the very low frequency perturbations, and the coupling of seismic noise for explaining the 10-20 Hz noise peaks.

We have now two quadrant diodes on all beams, allowing to exploit the whole available alignment information. However, not all give interesting signals in this moment.

The installation of galvo mounted mirror assemblies for fast auto-centering of the beams on the quadrant diodes is almost finished: Galvo systems have been installed in all beams, all electronics are ready and cabled, and one complete fast centering loop is working on the West end bench since several months without problems, improving the centering accuracy by more than a factor 100 with respect to the previous translation stage design.

Ongoing effort of optimization of the control filters for alignment and local control (for the mirrors under drift control, see 1.3.3) allowed to push the alignment noise below the theoretical sensitivity curve at almost all frequencies: see Figure 6. For some critical degrees of freedom we are now at the limit of optimization; for getting better cut-off (injecting less noise) we would have to reduce the low frequency gain (alignment precision). The already existing theoretical noise projections, assessing the impact of electronics noise (preamplifier, ADC, demodulator) and shot noise on the interferometer sensitivity, have been refined and explain well the alignment noise floor at higher frequencies. The new alignment electronics (quadrant diodes and demodulation boards, new ADCs) should further reduce the alignment noise floor and give additional margin for Virgo+.

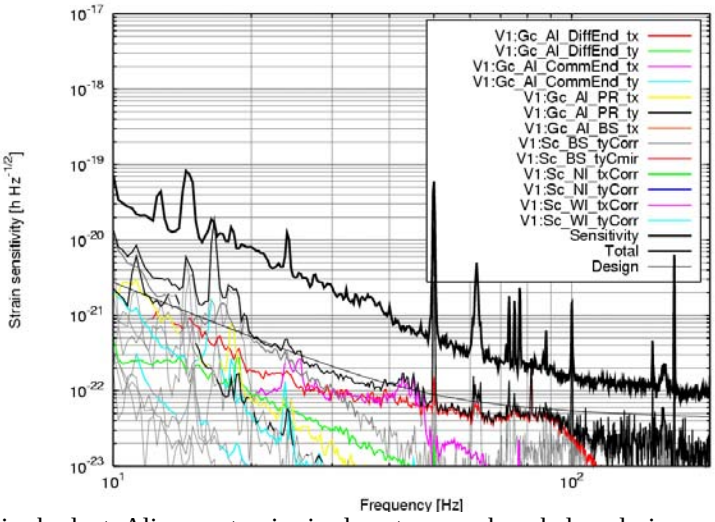

Fig. 6: Alignment noise budget. Alignment noise is almost everywhere below design sensitivity. The red curve (Differential End tx) has been pushed further down since the plot was taken.

Next plans

The most important change for Virgo+ is the change of the quadrant diode front-end electronic. Also new demodulation boards are under preparation, with lower noise and higher gain flexibility. The improvements on the ADC, demodulator and front-end electronic performances will bring a reduction of the alignment error signal electronic noise of about a factor of 3. The new global control system will have a big impact on alignment, allowing greater flexibility for the control architecture, higher sampling rate (lower delay, so more

flexibility for control filters), and better possibilities for change of control parameters on-the-fly.

3.3 Mirror suspension control

Mirror suspension control strategy underwent to a significant improvement during VSR1 resulting in a much more robust control in bad weather conditions and in the case of earthquakes. Just after the run MSC work-group tasks were mainly aimed to the stabilization of the suspension system disturbance rejection strategy and focused the efforts to the attempt of further improving Virgo sensitivity with mainly the improvement of the angular local controls and the reduction of the mirror actuation noise.

Local controls of the payload

We performed a study to infer any entry point of external disturbance or control noise that could be responsible of noise up-conversion in the critical region of Virgo best sensitivity, due to generic unknown coupling process. The only clear effect delineated was related to the noise injected by the local angular control of NI and WI mirrors in the bandwidth 1-3 Hz. Hence it was needed an improvement of NI and WI local control performance in order to reduce the gain demand to the automatic alignment of NE and WE and noise up-conversion in the Virgo sensitivity: the control filters have been improved as well as the electronics of the PSDs (dual dynamical range of the amplifiers). These improvements are summarized in Figure 7.

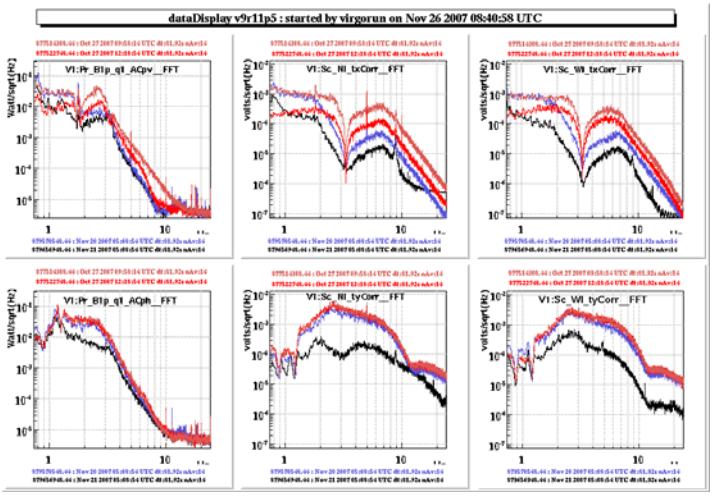

Fig 7: 2nd and 3rd columns:local control correction signals of the input mirrors during VSR1 (red) and now (black). First column: impact on the angular ITF signals used for the control of the end mirrors.

Actuator noise reduction and hierarchical control

The payload resonances (e.g. 16.7, 46.7 Hz) were seen in the Virgo sensitivity curve. These were due to the suspensions where marionette reallocation is implemented. A reshaping the marionette reallocation filter allowed a significant reduction of the impact of these resonances.

After several improvements in the low frequency part of the spectrum, there was the suspect of being limited by actuation noise coming from beam splitter and end mirrors. New measurements of the non-linear noise of DAC boards have been carried out, resulting in the

upper limit projection of the DAC noise shown in Figure 8 (left). To reduce the contribution of this noise two kind of actions have been performed

- At the beam splitter level, part of the longitudinal correction has been re-allocated to the marionette, with a strategy derived from the one already implemented at the end towers. The force applied to the reference mass was reduced by a factor 7. This allowed implementing a larger series resistor on the reference mass coils and a more aggressive emphasis filter.
- The end mirror coils have been equipped with 4 times larger series resistors and the control strategy has been modified to four coils per mirror instead of two. With these modifications the DAC noise is expected to be reduced by $4/\sqrt{2}$.
- The marionette coil drivers have also been modified with series resistors: the marionette DAC noise was found to limit the sensitivity at 10 Hz.
- New coil drivers with better filtering capabilities have been produced (4 boards) and successfully tested on the interferometer. These will be used with the smaller magnets on the end mirrors and provide an additional filtering of the DAC noise.

The estimate of the actuation noise in May 2008 is shown in Figure 8 (right) as well as the expected improvement with the new coil drivers (red curve).

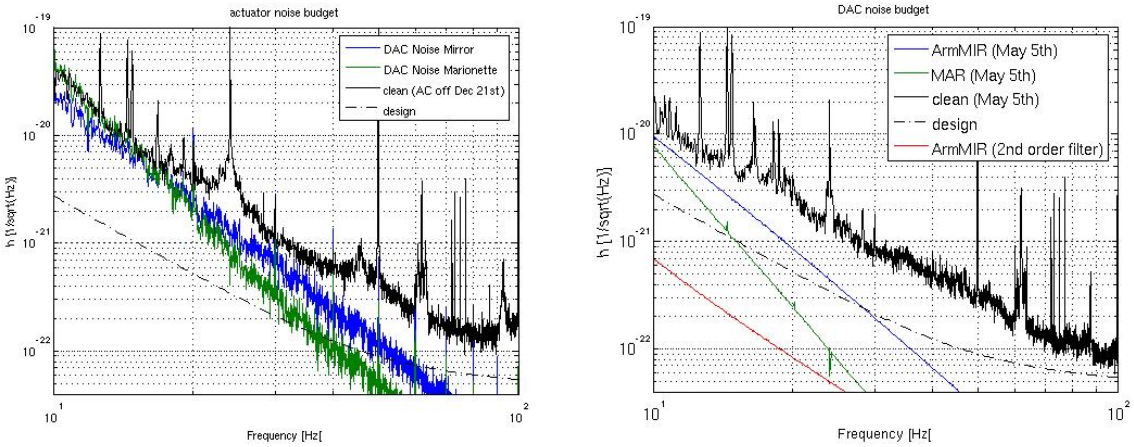

Fig 8: *Actuator noise including the non linear DAC noise before any modifications to the coil drivers (left, Dec 21st 2007) and after (right, May 5th 2008). The red curve on the right plot shows the expected DAC noise from the arm mirror actuators with the new coil drivers.*

3.4 Injection system

The injection system commissioning activities were mainly focused on the reduction of the coupling of environmental noises (beam jitter, scattered light): see 1.5.
A lot of effort was dedicated to prepare the upgrade of the injection system (see Detector report) whose installation is starting now. The plan for its commissioning is briefly described below.

Plans until VSR2

The planning for the installation and functional tests can be found in the Detector report. A provisional plan for the commissioning of the new injection system (ISYS) is the following:

1/ New input mode-cleaner end mirror local controls have first to be commissioned in order to be able to relock the input mode-cleaner. Mechanical transfer function of the new IMC end mirror will be measured and some new filters will be developed. This work is required to relock the IMC cavity and commission the ISYS.

2/ Once the upgrades on the laser are completed, the ISYS will be relocked with Virgo-like power (8 Watts at the output of the input mode-cleaner). For that it will be needed to

measure the control matrix of the different loops, develop some filters and close properly all the loops (mainly Beam Monitoring System, and ISYS Automatic alignment).

3/ Then the ISYS will be commissioned with the full power.

4/ We have to ensure that the injection system loops are able to work at every power in order to give the possibility to lock the ITF with different laser power to manage in a optimised way thermal effects that occurs in the ITF. The laser power will be tuned using a half-wave plate mounted on a remotely controlled rotator.

5/ Once the faraday isolator isolation optimisation upgrade is installed it will be commissioned. The faraday isolation will be checked (it should reach more than 30 dB of isolation) and the rotator calibrated.

4 Thermal effects and their compensation

4.1 Thermal effects studies

At the end of November 2007 the cleaning of the WI and NI mirrors was performed with the "first contact" polymer. The mirror showed few dust particles in the surface, but several white spots and translucent reflection of the intense illuminator light indicate the presence of water condensation contamination. Whenever at inspection the amount of particles and contaminations seemed lowered no evident benefit was exhibited by the interferometer. The typical signal of thermal transient did not show significant differences. The particular analysis of absorption carried out by measuring the temperature evolution of the mirror did not show clear benefit from the cleaning. Also the sidebands aberration measurement performed with the phase camera showed no significant improvement.

An Optical Simulation Group has been created, mainly devoted to characterize the interferometer in the different thermal states and with thermal compensation. The group selected Finesse as reference code for frequency domain simulations and decided to use DarkF both as an important counter-check code and as code for analysis in which high order aberration of optical components can play an important role like, as an example, the residual TCS aberrations. Among the result on interferometer characterization there are the identification of the cold-state aberrations as dominated by (small) astigmatism in the input beam and the clarification of the contribution of long arms in sidebands behavior, with a particular note to the long-arms cleaning effect which is presently under study for eventual application. Also the hot-interferometer working point has been better qualitatively established by completing Finesse simulations. The tightening of the collaborations among various groups allowed to approach the TCS simulation in a more efficient way: The C02 power distribution on the mirror has been simulated (using Zeemax) while DarkF has been extended to account for the C02 power distribution on the mirrors. Tests on double cavity system have shown good results and tests on the whole interferometer are presently under way. With respect to TCS experiment performed so far simulations show good agreement for the C02 power needed to correct the thermal lensing in WI mirror, as shown by the phase camera signals. It remains unclear and object of study the procedure to recover the “cold interferometer” state starting from the actual hot interferometer working point. The installation of the phase camera system should also help the understanding of the sidebands behaviour. This installation will be performed during the shutdown.

4.2 Thermal compensation

A description of the preparatory works for the thermal compensation system can be found in the Detector report. The TCS benches and in vacuum mirrors were installed mid-April at the

input mirrors. The commissioning of the TCS started with only WI test mass compensated (since only one laser was available). The choice for the WI is due to the fact that this test mass shows the highest absorption. Several tests have been performed:

- While the ITF was locked in low noise configuration the TCS was switched ON with several values for the CO_2 laser power. This always resulted in highly imbalanced sidebands. A good balancing could only be recovered by bringing the recycling cavity far from resonance
- The TCS was switched ON as soon as the ITF was locked on the dark fringe but the lock would not survive
- Finally it was decided to try to increase the input laser power together with the thermal compensation: while the interferometer was locked at step 12, the input power could be increased from 8.5 up to 9.25 Watts, while increasing the TCS power. The TCS power was set in order to keep the sidebands well balanced. Figure 9 shows the interferometer signals during this test. The power incident on the BS follows the input power as expected while the power on the dark fringe decreases; this might be due to the fact that the total aberrations increase since the NI was not compensated. As expected, the shot noise decreased and no noise injected by the TCS was observed (except for a line around 600 Hz): see section 1.6 for noise considerations. This successful trial is considered very encouraging.

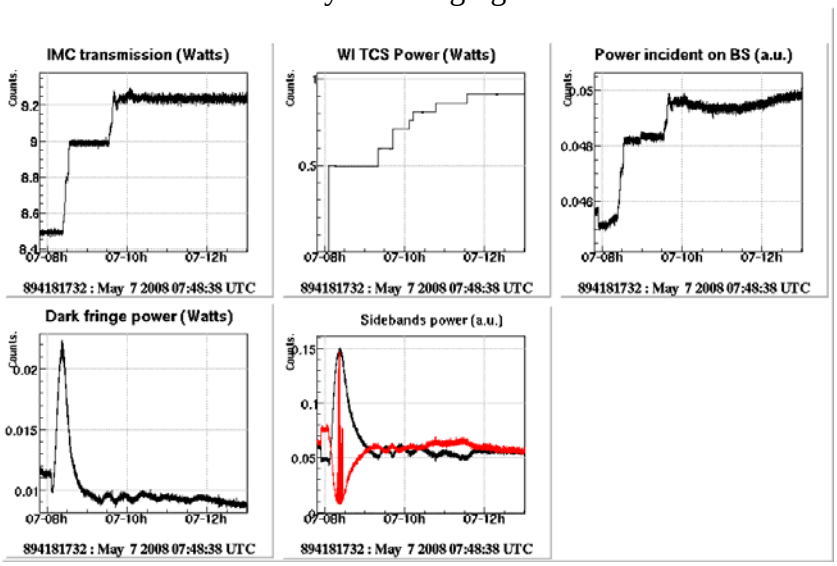

Fig 9: *Lock of the ITF with increasing input power ('IMC transmission') and with the thermal compensation on the WI mirror.*

The activity during the shutdown is mainly focused on the development of the intensity stabilization control loop for the CO_2 laser, in order to be compliant with Virgo+ sensitivity. The second laser, when available, will also be installed and aligned.

5 Noise hunting

Since the end of VSR1 a relevant fraction of commissioning time has been dedicated to environmental noise studies. These concerned the study of magnetic disturbances, and of the seismic/acoustic noise coupling to the ITF through scattered light processes. The investigations aimed to identify the major sources and coupling paths, as well as to measure the noise coupling and determine the noise contribution to the sensitivity. Mitigations actions were performed, and a significant improvement in the sensitivity has been achieved since the end of VSR1. More actions are planned for Virgo+.

5.1 Magnetic noise studies and reduction

The environmental magnetic field and gradient are expected to couple to the dark fringe through the mirror magnets, by exerting a torque or a force on the mirrors. The coupling would be larger on the two input mirrors which, by mistake, had the four magnets assembled in a parallel configuration.
The coupling of magnetic noise to each mirror has been measured by injecting intense magnetic fields at some frequency lines (5Hz to 100Hz) using one coil placed close to the mirror just outside the oven, and observing the effect in the interferometer. An unexpected high coupling was found with the field along the beam direction. From bench tests we observed that the aluminium bulk of the reference mass distorts magnetic fields and creates a magnetic gradient which is directed perpendicularly to the mirror and is quite intense at the position were the mirror magnets are located. This explains the high coupling for fileds along the beam direction. This also indicates that a dielectric reference mass can help to reduce the magnetic noise coupling.

In order to measure the TF of the environmental magnetic noise to the interferometer we made injections with the coil placed in the far field of the ITF and the magnetic sensors. From these measurements we derived a noise projection. Magnetic lines were clearly visible in the sensitivity and well predicted by the projection: the 50Hz line, a few lines around 10Hz, and a few sideband of the 50 Hz. The coupling of magnetic disturbances via the detection-lab electronics has also been measured and found negligible.

The overall coupling was reduced when the magnets of the input mirrors were replaced with weaker ones and with the anti-parallel polarity. The largest effect was observed when the lateral magnets of the NI were removed (a factor 5). The most recent noise projection is shown in Figure 10. The dominant contribution is now from the NE.

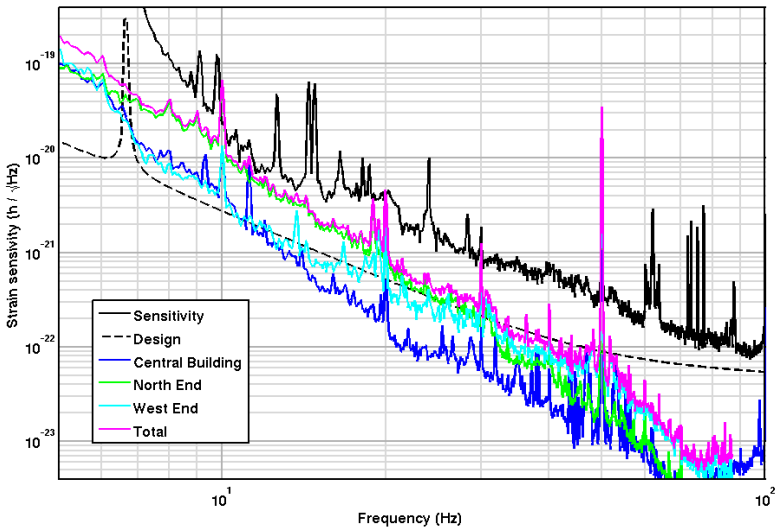

Fig 10: Estimated noise contribution of environmental magnetic fields of the Central, North and West experimental halls. The measurement error is a factor 3.

The noise from NE and WE is expected to be reduced by a factor 5 with the smaller magnets. Magnetic noise mitigations might nevertheless be necessary for Virgo+. The towers vacuum chambers and the oven do shield the mirror from the external magnetic field (we found they act with a pole or double pole at 5Hz, depending on the field directions). All sources located inside the oven have already been placed away. The environmental magnetic noise could also be reduced by moving the electronics racks away from towers.

5.2 Scattered light studies and reduction

At the end of VSR1 many of the structures limiting the sensitivity up to few 100Hz were due to noise from back scattered light and input beam jitter. This noise was sustained by seismic and acoustic environmental disturbances produced mainly from the air conditioning devices and the electronic racks. We worked on the reduction of the environmental noise in the halls and on the reduction of the coupling to the dark fringe (scattered light and beam jitter).

5.2.1 Noise sources

By means of switch off tests the noisiest devices and the main noise paths have been identified. Figure 11 shows the result of one test performed in November 2007 when all air conditioning devices were progressively switched off. This revealed significant contributions from all air conditionings and one water pump. We also found that the electronics racks located inside the laser lab are responsible for some noise lines around 200Hz and 400Hz.

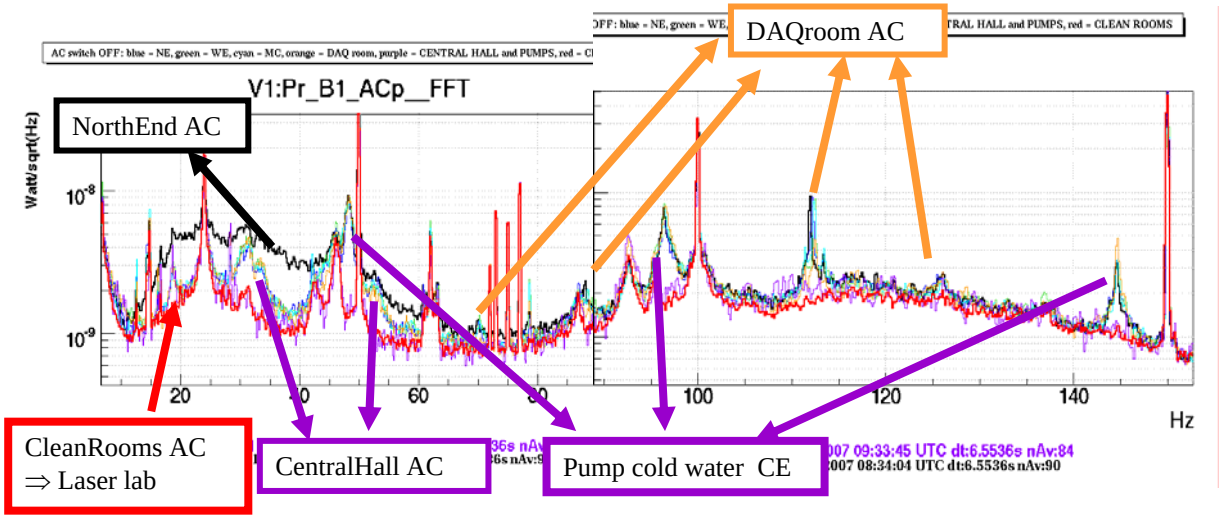

Fig 11: Reduction of noise in the dark fringe photodiode correspondent to the progressive switch off of all HVAC devices (November 2007). The air conditioning inside the laser laboratory is responsible for noise at low frequency; the central hall HVAC is responsible for a broadband structure around 30 Hz and lines at the pump harmonics (48, 96 and 144 Hz); that of the DAQ room is responsible for a broadband noise up to 200 Hz; the end buildings HVAC create a broad band noise (up to ~100Hz).

Several works have been performed to reduce the noise emissions from these devices, additional works are to be performed during this summer:

- The noise from the DAQ room has been reduced by (i) installing a new air conditioning machine outside the room, further away from the experimental hall, and (ii) acoustically isolating the room in order to filter the noise from the racks. Acoustic and seismic noise reduced significantly between 30 and 200Hz inside the room (factor 5) and in the hall.
- The End benches acoustic isolation has been improved, resulting in a slightly better shielding from HF acoustic noise.
- The noisy water pump (recycling pump of the cold water for the Central hall HVAC) has been kept off during the winter season. To cope with the higher thermal load of the summer season it should be possible to compensate with the upstream pumps located in the technical building.
- The laser lab racks will be moved to another room, acoustically shielded.
- The control of the air conditioning of the laser lab will be separated from that of the clean rooms. The air flux will be improved and could be adapted to the reduced conditioning needs when the electronics racks will be moved.

- We will try to reduce the noise from the central hall air conditioning by (i) reducing the air flux (new fans and motor), (ii) inserting bellow dampers between the machine and the air pipes to reduce their vibrations, (iii) adding silencers.

5.2.2 Coupling to the dark fringe

Several actions helped to reduce the coupling of environmental seismic/acoustic noise through scattered light processes, leading at the end of April to a horizon distance steadily above 6Mpc. The input beam jitter has also been well reduced above 100 Hz.

1) Detection port: Brewster and suspended detection bench

The seismic and acoustic noise inside the central hall was suspected to couple through scattered light at the detection port (either inside the detection tower or at the Brewster link): there was good coherence with seismic sensors placed there and this area was very sensitive to tapping tests. This noise (structures from typically 100Hz to 500Hz) was strongly non stationary, and highly dependent on alignment fluctuations and weather conditions: its amplitude was found to vary with the dark fringe power.

The detection tower was addressed first. The main mitigation works were: (i) damping the secondary beams created by AR coated surfaces of the OMC, mirrors and lenses; (ii) insertion of a very large baffle covering the detection tower west wall to damp possible parasitic beams; (iii) upgrading the design of absorbing glass baffles and diaphragms placed inside the Brewster link to minimize the light back-scattered from the Brewster window or the detection optics. No significant improvement has been observed after all these operations.
The Brewster link remained the only suspect. In March 2008 the Brewster was replaced with a cryogenic tube (see Detector report). The characteristic noise structures disappeared from the dark fringe and the noise stationarity remarkably improved (the horizon kept steadily above 5Mpc also during bad weather). It is not yet clear which through which mechanism this noise coupled to the dark fringe.

The remaining peaks in this region (158Hz, 266Hz) have been associated to the suspended detection bench optics and indicate a residual back-scattered light noise at the detection port. It also remains to be addressed a possible noise associated to the detection tower output window.

2) Scattered light on external benches

The AC off tests indicated the presence of up-converted noise up to at least 50Hz, which seemed correlated to the seismic noise of external optical benches. We installed 3-axial LF seismometer on each external bench in order to have a good monitoring of the bench displacements. We thus discovered that all benches have the largest displacement in correspondence to the 10-20Hz horizontal resonances of the support structure and legs. We excited these resonances using a commercial shaker placed on the bench and found clear evidence of up-converted noise limiting the sensitivity up to about 100Hz. All benches seemed to contribute. The noise is explained reasonably well by light that is phase modulated by a seismically excited surface and recombined in the ITF. Figure 12 (left) shows the projection of up-converted noise from each bench derived from this model (tuned with the measurements).
All benches have been thoroughly checked for diffused light sources. Several critical elements were identified with tapping tests. Most effective cures consisted in cleaning of the optics and the replacement of beam dampers with better ones (absorbing glass when possible). Figure 12 (right) shows the noise projection after this mitigation: a factor 2 to 6 reduction of the up-

converted noise, depending on benches was obtained. A reduction of noise was also observed in the longitudinal and in some alignment error signals. Figure 13 shows the sensitivity improvement (this includes also the Brewster removal). There is a clear gain up to 100Hz.

The residual noise is still slightly above the Virgo design and further improvements are planned:

- Damp the horizontal resonances (around 20 Hz) of the optical benches. A resonance damper prototype has already been produced and successfully tested. A reduction of the resonance amplitude by a factor 3 to 4 could be obtained. Such dampers are in preparation in order to equip all benches after the shutdown. The option to stiffen the legs structure will also be tested. More invasive and expensive options are being evaluated for the future, like air spring legs or active damping
- Part of the scattered light on the end benches is due to spurious beams originating from multiple reflexions inside the end test mass which is not coated. The new NE mirror will be produced with an AR coating on its back face. Its transmission will also be reduced by a factor 4.
- Care will be taken to reduce diffused light when replacing the injection bench optics and the diffused light will be further reduced on the other optical benches. Laboratory measurements of the light scattered by different types of beam dumps, photodiodes and optics are in progress. This should guide the improvement of the optical setups.

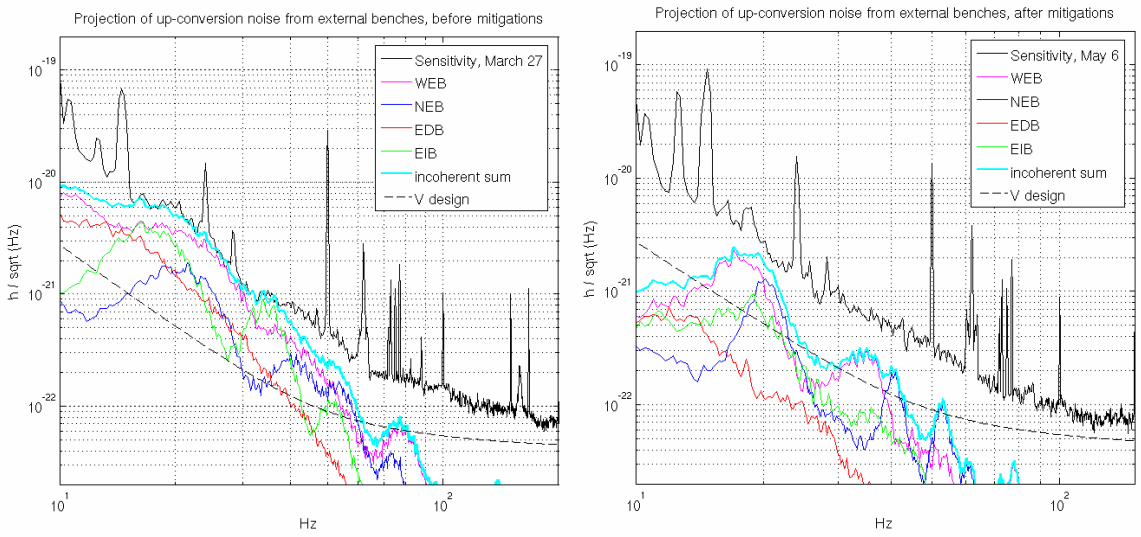

Figure 12: Noise from diffused light at the external optical benches (end stations, detection and injection). Left: the situation before the diffused light mitigations, right: same after the works. The color curves show the phase noise from light backscattered by a surface moving with the bench. This noise is predicted for each bench by tuning the model parameters with the noise produced when the bench is shaken. In cyan is the incoherent sum.

3/ Scattered light inside the arm tubes

A campaign of measurements has also been done in order to characterize the effect of scattered light inside the vacuum tubes. Shaking of the tubes was performed at the location of the input, intermediate and end baffles. No effect was observed on the dark fringe and an upper limit of this effect was placed. This upper limit is compatible with the Advanced Virgo design.

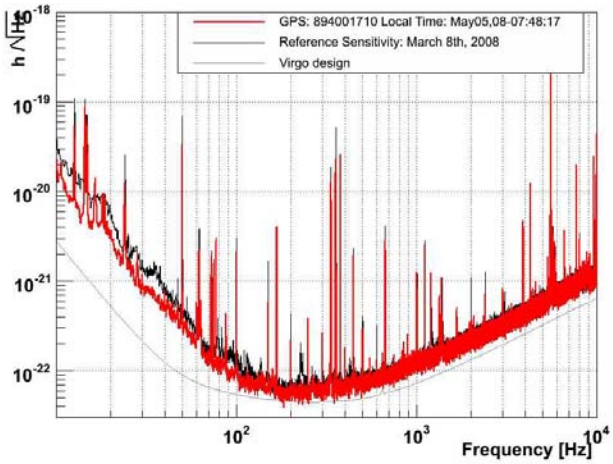

Fig 13: *Sensitivity improvement after the Brewster removal and the optical benches mitigations.*

4/ Input beam jitter reduction

As foreseen in the last report, the Beam Monitoring System (BMS) piezos and mounting system located on the injection bench has been changed to reduce the remaining contributions BMS resonances (beam jitter) in the dark fringe. In figure 14 on the picture, the new BMS piezo and mounting system is shown in its 2 inches version.

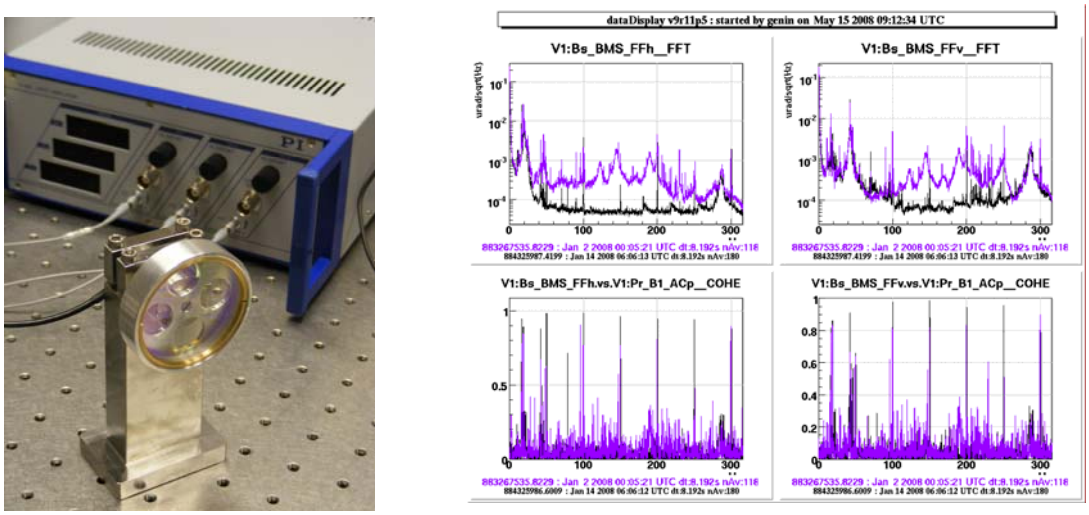

Fig 14: *picture : new BMS piezo and mounting and the associated electronics; right plot : beam jitter and coherence with dark fringe(purple: old BMS; black: new BMS).*

The input beam has been reduced between 40 and 260 Hz by more than one order of magnitude on almost all this frequency bandwidth as shown in Figure 14. The coherence between dark fringe and input beam jitter has also been reduced in correspondence to the mechanical resonances of the former BMS system.

6 Noise budget and foreseen improvements

Figure 15 shows the most recent noise budget (without thermal compensation). The sensitivity is well explained by control noises and by shot noise below 20 Hz and above 150 Hz. In the intermediate region a large fraction of the noise could occur from the Eddy currents but this could not be demonstrated before the shutdown (due to the incident at NE). It should

be noticed that in this region many noises are expected to be at the same level as the Virgo design (magnetic noise, scattered light, control noises) and could add up to a non negligible contribution to the sensitivity. The environmental noises are not yet included in this noise budget: see Figures 10 and 12.
It is worth mentioning that the thermal compensation system should help in the reduction of some noises: with a good thermal compensation the sidebands will have a higher recycling gain (it should be about a factor 3 higher without thermal effects), therefore, for the error signals limited by readout noise (shot noise or electronic), the signal to noise ratio should be increased and the impact on dark fringe accordingly reduced. This is the case for the B1 electronic noise, the frequency noise (B5 shot noise) and some of the alignment error signals. These improvements could not be verified since only a partial thermal compensation could be performed.
Similarly the increase of the input power will reduce the impact of electronic noises.

6.1 Noise budget with P_0 = 8 Watts

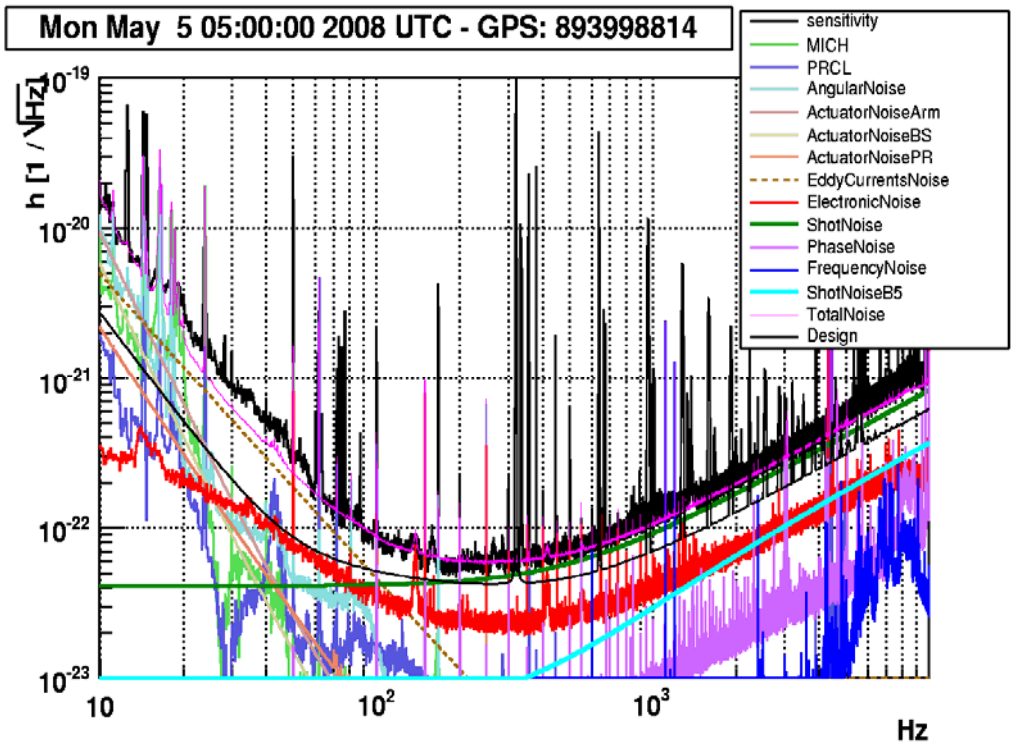

Fig 15: *Recent noise budget with input power P_0=8Watts. The total noise (pink curve) also includes the expected thermal (pendulum and mirror) noises.*

Shot noise

Above 200 Hz the sensitivity is mainly shot noise limited (green curve). The shot noise is computed using the power measured on the dark fringe and the measured optical gain. It corresponds, within better than 10%, to the expected shot noise for an input power of 8 W, a recycling gain of 43 and a transmission to the dark fringe photodiodes of 80% (losses and mismatching of the output mode cleaner and losses of the Faraday isolator).

Other high frequency noises: frequency noise and B1 electronic noise

The laser frequency noise (dark blue and light blue) is now limited by the shot noise of the error signal (B5 photodiode). It usually sits well below the Virgo design except when its

coupling to the dark fringe is too large (mainly due to the etalon effect). This effect can nevertheless be controlled as discussed in section 1.3.4 of the October 2007 report. A dedicated control of the Etalon effect should be defined and put in operation after the shutdown.
The B1 electronic noise (red curve) is quite high but its impact should be reduced when the TCS will be put in operation and with higher input power.
At present, the frequency noise and the B1 electronic noise are responsible for an increase of the noise at high frequency by 25 to 30% with respect to pure B1 shot noise.

Angular and longitudinal control noises

The noise introduced by angular and longitudinal control loops (MICH, PRCL) limits the present sensitivity only below 20 Hz (see Section 1.3) and is close to the Virgo+ design up to 100 Hz. Some of the error signals are limited by electronic or shot noise and their impact will be reduced with the TCS and an increased input power. Others are limited by environmental noises (beam jitter and diffused light) and these will be addressed during Virgo+ commissioning.
The electronic (DAC) noise of the mirror actuators might limit the sensitivity around 10 Hz (maroon lines give upper limits). The new coil drivers with better filtering capabilities have been put in operation on the end mirrors just before the incident at NE. With these coil drivers the actuator noise should be compliant with the Virgo+ design at 10 Hz (see section 1.3.3).

Eddy currents noise

The increase of the pendulum thermal noise related to the Eddy currents dissipation in the reference mass (maroon dotted line) is an upper limit. The input mirrors' magnets have been replaced with smaller ones (5.5 times less strong) but no reduction of noise was observed. It was realized later that the sensitivity was limited by noise from diffused light below 100 Hz (see 1.5), hiding possible reduction of Eddy currents noise. Then the magnets of the end mirrors have also been replaced but the incident at NE prevented to check the effect.

Diffused light and beam jitter

These noises are not yet included in the Virgo noise budget due to the difficulty to model them and their non stationarity. The diffused light from the external optical benches has been well reduced but still contributes below 50 Hz (see section Figure 12). The noise suspected to be related to the Brewster window (100-200Hz region) has completely disappeared. A small contribution from the suspended output bench is visible at 155 Hz. Investigations are going on to understand the source of this noise.
There is no more contribution from beam jitter except may be the peaks below 20 Hz (injection bench resonances).

Magnetic noise

Magnetic lines are still visible in the dark fringe (around 10 Hz and 50 Hz). The magnetic noise from the end buildings is still above the Virgo+ design (see Figure 10). However, it should be reduced by a factor 5 with the use of smaller magnets which should be enough to reach the Virgo+ design.

6.2 Noise budget with thermal compensation on the WI mirror and P_0 = 9.25 Watts

Figure 16 shows the noise budget obtained with the thermal compensation on the WI mirror (0.7 Watts) and an input power increased from 8 to 9.25 Watts. The shot noise computed from the measured B1 power and optical gain decreased by 7% as expected. Unfortunately, since the compensation was applied only on one input mirror and the input power was increased the aberrations were probably larger, resulting in a decrease of the sidebands power and therefore a higher impact of the B1 electronic noise (see red curve). As a result the sensitivity was not

visibly improved at high frequency. The noise induced by the TCS CO_2 laser (purple curve) was not limiting the sensitivity except for some lines (50 Hz harmonics and 595 Hz line) but, as expected a CO_2 power stabilisation will be needed to reach Virgo+ design.

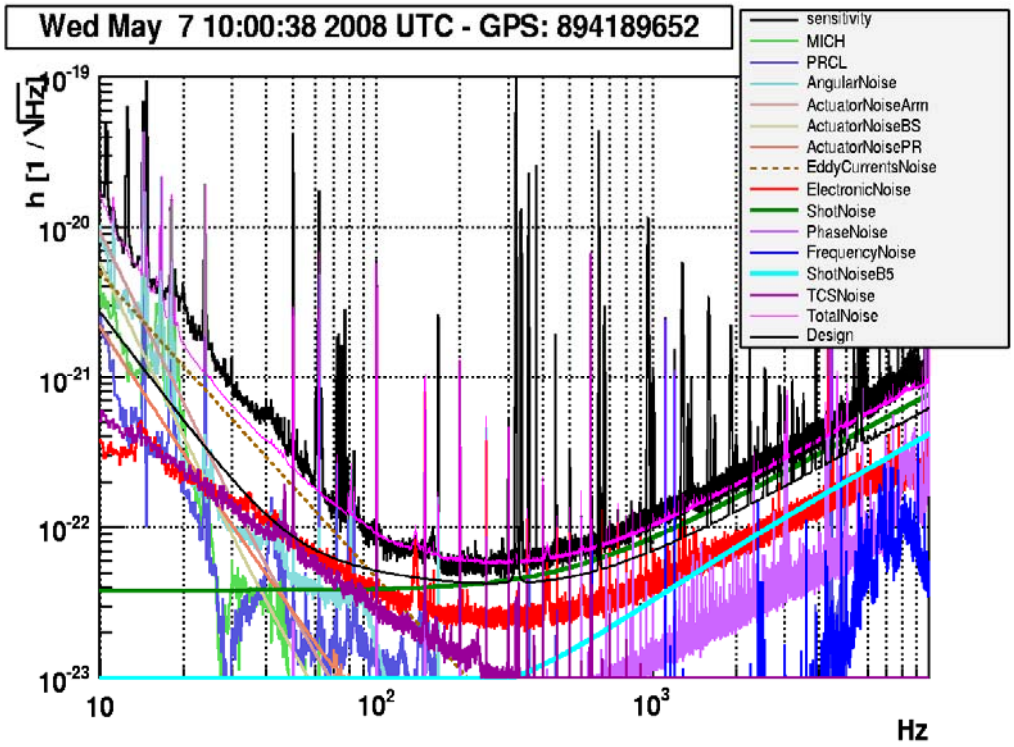

Fig 16: *Noise budget with the thermal compensation on the WI mirror and an input power P_0=9.25Watts. An estimate of the noise induced by the CO_2 laser is included (denoted TCS noise).*

7 Short term plans: from the Virgo+ shutdown to VSR2

The commissioning of the full interferometer should restart in September 2008, after the upgrade of the injection system, the installation of the new control electronics and the replacement of the NE mirror (see Detector report for details and a complete list of the shutdown activities and upgrades). The commissioning of the new injection system in standalone will be performed during the summer as well as functional tests of the new control electronics. The complete phase camera system will also be installed this summer.

First the injection system will be characterized. The input beam will be aligned and matched to the Fabry-Perot cavities. The north cavity will also have to be aligned and characterized.

Then the interferometer will be relocked with low input power (8 Watts) and with the old control electronics. The controls should be retuned to work with the smaller end mirror magnets and the new coil drivers. The noise budget will be checked (effect of smaller magnets, status of control and environmental noises). A sensitivity as good as before the shutdown should be restored as a first step. The noise levels of the new injection system will have to be carefully checked. The new control electronics system will not yet be used but it can be validated during this period since it partly can run in parallel with the old one.

Then the commissioning of the interferometer with the TCS will restart with the compensation on both input mirrors. If it turns out that a good compensation cannot be

obtained starting with 8-10 Watts the ITF will be locked with only few Watts and the input power slowly increased together with the thermal compensation. This will require ensuring that the control loops work in a wide range of input power.

When the thermal compensation will be working with 8-10 Watts of input power the new control electronics will be put in operation step by step as described in section 1.3.2.

The hunt for environmental noises (magnetic noise, diffused light, beam jitter) will go on in parallel with the commissioning of the thermal compensation.

Once the new control electronics will be put in operation the increase of the input power will restart with the thermal compensation.